

Velocity dependence of the cross section for Penning and associative ionization of argon atoms by metastable neon atoms

A. AguilarNavarro, B. Brunetti, S. Rosi, F. Vecchiocattivi, and G. G. Volpi

Citation: *The Journal of Chemical Physics* **82**, 773 (1985); doi: 10.1063/1.448502

View online: <http://dx.doi.org/10.1063/1.448502>

View Table of Contents: <http://scitation.aip.org/content/aip/journal/jcp/82/2?ver=pdfcov>

Published by the AIP Publishing

Articles you may be interested in

[The stereodynamics of the Penning ionization of water by metastable neon atoms](#)

J. Chem. Phys. **139**, 164305 (2013); 10.1063/1.4826101

[Absolute metastable atom-atom collision cross section measurements using a magneto-optical trap](#)

Rev. Sci. Instrum. **78**, 073102 (2007); 10.1063/1.2754444

[Coherent control of collision processes: Penning versus associative ionization](#)

J. Chem. Phys. **125**, 094315 (2006); 10.1063/1.2336430

[Absolute Doubly Differential Electron Bremsstrahlung Cross Sections from Free Atoms](#)

AIP Conf. Proc. **680**, 115 (2003); 10.1063/1.1619678

[Energy dependence of the Penning ionization electron spectrum of \$\text{Ne}^*\(3s\ 3\text{P}\ 2,0\) + \text{Ar}\$](#)

J. Chem. Phys. **118**, 3124 (2003); 10.1063/1.1536615



Velocity dependence of the cross section for Penning and associative ionization of argon atoms by metastable neon atoms

A. Aguilar-Navarro,^{a)} B. Brunetti, S. Rosi, F. Vecchiocattivi, and G. G. Volpi
Dipartimento di Chimica, Università di Perugia, 06100 Perugia, Italy

(Received 5 June 1984; accepted 1 August 1984)

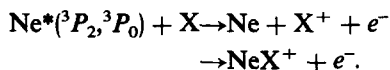
Relative cross sections for Penning and associative ionization in $\text{Ne}^*(^3P_{2,0})\text{-Ar}$ collisions have been measured, in a crossed beam experiment, as a function of the collision velocity, in the thermal energy range. The total ionization cross sections have been analyzed, together with other experimental results, obtaining a best fit resonance width function. The analysis of the associative to Penning ionization cross section ratios shows that, in the high collision energy range, the ionization occurs predominantly through the $^2\Sigma_{1/2}$ ground state of NeAr^+ ion. Some considerations on the role played by the interaction anisotropy in these ionization processes are reported.

I. INTRODUCTION

In the thermal energy collisions between two atoms, when one is electronically excited at an energy higher than the ionization potential of the other one, ionization can occur. These processes have received much attention in the recent years.¹ Actually, because of their large cross sections, they play an important role in several phenomena such as, electrical discharges, thermal plasmas, and laser systems. In addition to their importance in practical applications, these ionization reactions are also studied in view of their general interest in the field of the excited state chemistry.² Moreover these processes are characterized by the presence of a discrete state embedded in a continuum of states, and this aspect is rather interesting from a theoretical point of view.³

Most of the studies about ionization in thermal energy collisions of excited atoms have dealt with metastable $\text{He}^*(2^3S, 2^1S)$ atoms because of the ease of their preparation and state selection and their large importance in many systems. In fact, the high electronic energy of these atoms emphasizes the ionization channels in quenching processes.²

The metastable $\text{Ne}^*(^3P_2, ^3P_0)$ atoms have also enough energy (16.62 and 16.71 eV, respectively) to ionize many targets in thermal energy collisions.⁴ When they collide with heavier rare gas atoms, X, two ionization processes are possible:



The first one is usually called Penning ionization, while the second one, associative ionization. In the 1971 Cermak and Ozenne⁵ studied these processes measuring the energy spectra of the electrons ejected in the collisions between metastable neon atoms and heavier rare gases. In the same year Tang *et al.*⁶ reported the velocity dependence of total ionization cross sections for the same systems. Micha *et al.*⁷ proposed a two state model for the theoretical description of these processes, while Olson⁸ has made a classical calculation of the ionization cross section for the metastable neon-argon system. Neynaber and Magnuson^{9,10} measured the velocity de-

pendence of the Penning and associative cross sections by the merging beams technique. West *et al.*⁴ measured the absolute value of the total ionization cross sections and the Penning to associative branching ratios in a crossed thermal beam experiment. Recently Gregor and Siska¹¹ obtained the interatomic potentials from differential scattering cross sections for collision of metastable neon with heavier rare gas atoms.

The ionization processes of metastable neon atoms with rare gases show many interesting aspects. These atoms are in a *P* state, therefore their interaction with the collision partner is represented by a manifold of potential curves.¹² Moreover the exit channel is characterized by the ionic state of the target, which is also a *P* state. This leads to consider the ionization of a ground state rare gas by metastable neon as the result of several state to state processes. Recent works provided interesting contributions to the clarification of the problems connected with the ionization dynamics of these systems. Morgner¹³ proposed some selection rules which appear to govern the transitions from the neutral to the ionic states and Hotop *et al.*¹⁴ have shown the importance of the symmetry of the entrance channel to describe this type of process. However more experimental information is still necessary for a better understanding of the matter.

In this paper we report the energy dependence of the Penning and associative ionization cross sections measured for collisions of metastable Ne with ground state Ar atoms at thermal energies. The cross sections have been measured in a crossed beam apparatus using time-of-flight velocity selection. The energy dependence of the branching ratio has been measured accurately and compared with the results obtained by Neynaber and Magnuson in a merging beam experiment.⁹ A comparison is made also with other unpublished results,^{15,16} which show some discrepancies with the earlier data in the low energy region. A semiquantitative analysis has been performed in order to obtain information about the ionization dynamics. The analysis of the associative to Penning ionization cross section ratio, in terms of the potential energy curves involved, has been performed to date only for the $\text{He}^*(^3S, ^1S)\text{-Ar}$ system. The present work represents a first attempt of interpretation of the branching ratios for ionizations which involve metastable *P*-state atoms.

^{a)} On leave from Departamento de Química Física, Universidad de Barcelona, Spain.

II. EXPERIMENTAL

The crossed beam apparatus has been described in detail elsewhere.¹⁷ Some general features of the experiment are given here. A metastable neon beam crosses an argon beam at 90°. All the ions produced in the crossing region are extracted by an electric field, focused by a lens system, mass analyzed, and then detected.

A schematic view of the experimental set up is shown in Fig. 1. The metastable neon beam is produced by 500 eV electron bombardment of an effusive ground state neon beam. The neon beam source temperature can be adjusted from room temperature up to 650 K by a thermostatic device, in order to vary the velocity distribution of the metastable atoms. All the ions and highly excited Rydberg atoms produced by the exciter are removed from the beam by an electric field of 1500 V/cm. The metastable atom beam in the present experiment is expected to have a statistical mixture of $J = 0$ and $J = 2$ states.⁶ The argon beam is obtained by effusion from a microcapillary array at 300 K.

The metastable atoms are detected by a channel electron multiplier placed along the beam direction, behind the beam crossing center. The ions are extracted at ~ 150 eV and focused by an electrostatic lens into a quadrupole mass spectrometer, and then detected by a channel electron multiplier. To calibrate the mass scale and the detection efficiency as a function of the ion mass, some reference electron impact mass spectra have been measured using the electron gun located above the ion repeller. To avoid experimental errors due to different ion transmission throughout the mass spectrometer, the NeAr⁺ to Ar⁺ ion intensity ratio has been obtained also extrapolating the current ratio for the two mass numbers at zero resolution.

The velocity selection has been obtained using the time-of-flight technique. The primary beam is chopped by a slotted rotating disk 17 cm before the crossing center. The out-

put pulses from the two channel electron multipliers are sent to a time to amplitude converter which is started by a photo-cell signal from the slotted rotating disk. The amplitude converted output pulses are stored in a multichannel analyzer. In this way time spectra of the metastable atoms and of the product ions are obtained. The cross sections can be obtained from these time spectra by a numerical deconvolution procedure described in detail elsewhere.¹⁷ The velocity resolution for the metastable atoms ranges from about 10% to about 30% going from lower to higher velocities.

The associative to Penning cross section ratio is obtained with a better accuracy than the single cross sections because the ratio comes directly from the production time spectra of the NeAr⁺ and Ar⁺ ions, without any deconvolution procedure. In other words, the associative to Penning cross section ratio is obtained for a given collision energy, by the counting rates from NeAr⁺ and Ar⁺ ions at the corresponding delay time. Two typical time spectra, one for NeAr⁺ and the other one for Ar⁺, are reported in Fig. 2. The time scale has been corrected for the different ion flight times throughout the mass filter.

The measured cross section for a given metastable atom velocity v_1 is averaged over a relative velocity distribution due to the velocity resolution of the time of flight device for v_1 and the Maxwellian distribution of the target atoms. The most probable relative velocity is approximately given by $v_w = (v_{1w}^2 + v_{2w}^2)^{1/2}$, where v_{1w} and v_{2w} are, respectively, the most probable velocities of the metastable atoms for a given delay time and of the target atoms. The effective cross sections are given by

$$\sigma_{eff}(v_w) = \int_0^\infty \int_0^\infty S(v_1) \sigma(v) f(v) dv_1 dv.$$

$S(v_1)dv_1$ is the v_1 distribution function for a given delay time, determined by the gate function of the time-of-flight disk¹⁷; $\sigma(v)$ is the center of mass cross section for a relative velocity v ; for a right angle crossed secondary beam with a Maxwellian velocity distribution, $f(v)dv$ is given by¹⁸

$$f(v)dv = \frac{4}{\sqrt{\pi}} \frac{v}{v_1} x^2 \exp(-x^2) dx,$$

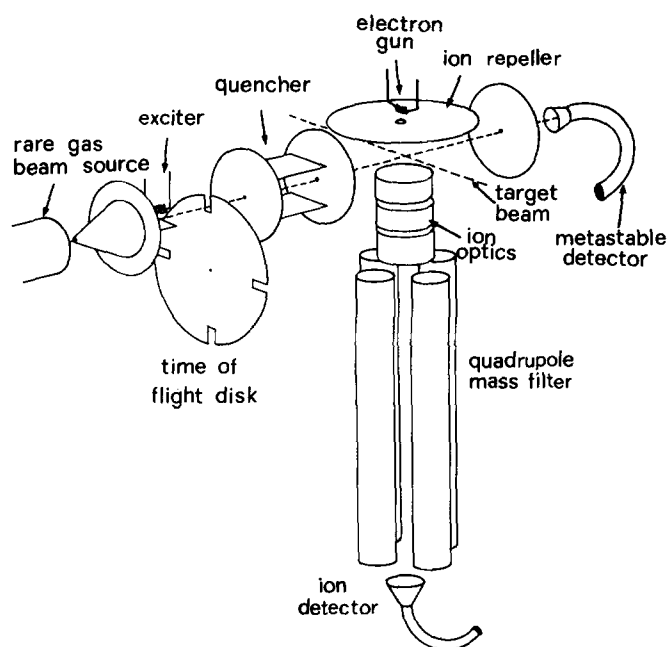


FIG. 1. Schematic view of the experimental setup.

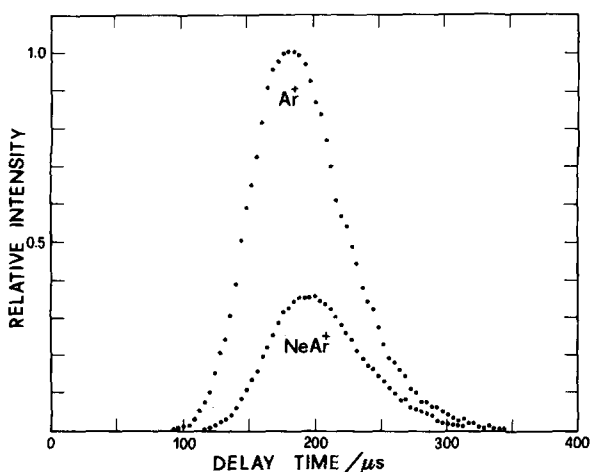


FIG. 2. Typical time spectra for Ar⁺ and NeAr⁺ product ions.

where $x = v_2/v_{2w}$, with $v_2 = (v_2^2 - v_1^2)^{1/2}$ and $v_{2w} = (2kT/m)^{1/2}$; T is the target beam temperature and m the target molecule mass.

To study how this convolution can modify the energy dependence of the experimental data, we have simulated experiments with several resolution conditions. We have observed that, for the Ne*-Ar system, the total ionization cross section is not sensitively affected by the convolution, while some effects can be presented on the associative to Penning cross section ratio which decreases drastically with the collision energy. In this case the shape of the branching ratio energy dependence can be modified by the convolution, especially in low velocity resolution experiments, for instance when a scattering chamber is used in place of a target beam or when the beam crossing region is not well defined so that averaging due to the angular spread of the two beams could be also present. For the present experiment the resolution conditions have been chosen to produce small effects on the branching ratios. Nevertheless during the analysis of our data, we have compared the experimental cross sections with those calculated in the center of mass system and convoluted according to the above procedure.

III. RESULTS AND ANALYSIS

The total, Penning and associative relative ionization cross sections for Ne*-Ar collisions, are reported in Fig. 3. The Penning to associative cross section ratios are shown in Fig. 4. For the cross sections and for the cross section ratios the collision energy range is not exactly the same because the cross sections of Fig. 3 are obtained by a numerical deconvolution procedure¹⁷ which cuts the velocity distribution tails.

A. The total ionization cross section

The energy dependence of the present total ionization cross section and those previously reported by Tang *et al.*⁶ and by Neynaber and Magnuson⁹ are in good agreement. Gregor and Siska¹¹ from the analysis of their differential

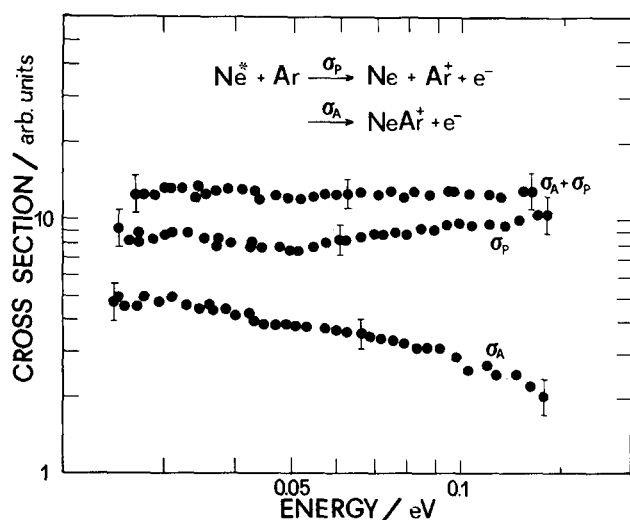


FIG. 3. Relative cross sections for total, Penning, and associative ionization in Ne*-Ar collisions, as a function of the relative energy. The bars show the size of the statistical errors.

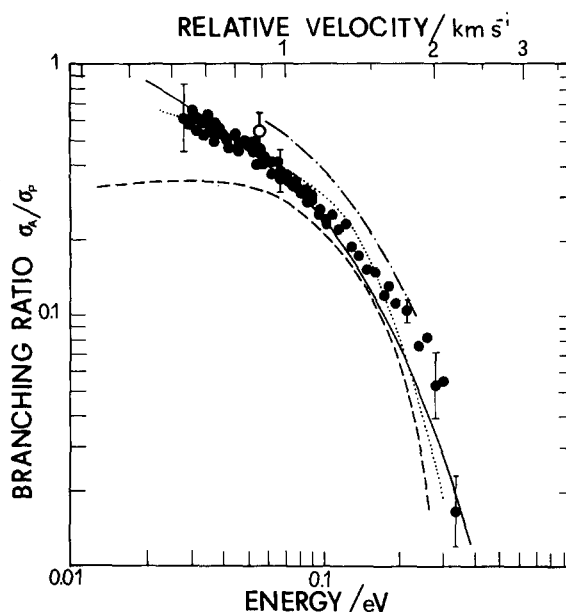


FIG. 4. Associative to Penning ionization cross section ratio for the Ne*-Ar system, as a function of the relative collision energy. The open circle is the ratio measured by West *et al.* (Ref. 4). The other curves are the fits of previous results: --Neynaber and Magnuson (Ref. 9); - - Kaufhold (Ref. 15); ... Gerard (Ref. 15); — Chen (Ref. 16).

scattering cross sections, of the experimental quenching rate constant at 300 K¹⁹ and of the total ionization cross sections by Tang *et al.* and by Neynaber and Magnuson in the 0.01–0.10 eV energy range, have obtained the interaction potential, $V_+(R)$, between Ne* and Ar, and the resonance width $\Gamma(R)$. Because the range covered by our branching ratios is 0.02–0.35 eV, we have extended the fitting analysis of the above experimental cross sections, together with our experimental results, up to 1 eV, in order to obtain a reliable resonance width $\Gamma(R)$ over a more extended energy range. Actually the total ionization data by Neynaber and Magnuson cover an even more extended range (up to 600 eV), but we limited our analysis to the above interval. The present relative cross sections and the earlier ones have been normalized to the absolute value measured for a collision energy of

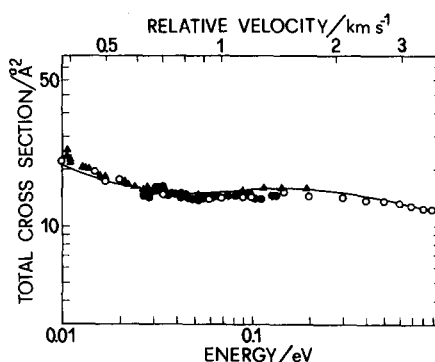


FIG. 5. Total ionization cross sections for Ne*-Ar collisions, as a function of the relative energy. Full circles are the present data, open circles are the data by Neynaber and Magnuson, and the triangles are the results by Tang *et al.* The line is the fit obtained using the $V_+(R)$ by Gregor and Siska and adjusting the parameters of $\Gamma(R)$ (see the text).

~ 0.056 eV by West *et al.*⁴ These cross sections are shown in Fig. 5 where the very good agreement of the relative energy dependence among all the experimental data is evident. This normalization gives reliable cross section values, in fact the integration over a Boltzmann distribution gives a rate constant at 300 K of 1.47×10^{-10} cm³/s, which is very close to the experimental value¹⁹ as reported in Ref. 11. The total cross sections reported in Fig. 5 have been fitted using the $V_*(R)$ potential by Gregor and Siska, assuming for the resonance width the usual parametric exponential form

$$\Gamma(R) = A \exp(-sR)$$

and adjusting the s and A parameters. These cross sections have been calculated within the "classical approximation"²⁰ which is known to be satisfactory for this system.¹ The best fit has been obtained for $s = 1.643 \text{ \AA}^{-1}$ and $A = 0.214$ eV.

B. The branching ratio

In Fig. 4 the present associative to Penning ionization cross section ratios are compared with the merging beam results by Neynaber and Magnuson,⁹ with the data from the Freiburg laboratory¹⁵ and with the data obtained by Chen.¹⁶ The Freiburg data have been obtained in two time-of-flight experiments: one using a pulsed electron bombardment exciter and another one using a mechanical beam chopper. Chen's data have been obtained in an experiment with crossed supersonic beams at controlled energy. Our data are in good agreement with the Freiburg results, while the Chen's data appear higher but with the same trend. The Neynaber and Magnuson branching ratios are systematically slightly lower at high and intermediate energies, but with a different trend in the low energy range where the merging beam data are affected by a larger uncertainty. The ratio obtained by West *et al.*⁴ for an average collision energy of ~ 0.056 eV, is also in good agreement with our data.

Quantitative analysis of the associative to Penning branching ratio, in order to obtain information about the potential energy curves involved, has been accomplished up to date only for the He*-Ar system.²¹⁻²³ These studies have been carried out assuming that the ionization processes can be described by a simple two state model.²⁰ According to this model, in a classical representation, at a given collision energy E and for a given impact parameter b the associative ionization is the result of those transitions occurring at interatomic distances between the turning point and a limiting distance R_{ai} such that

$$V_*(R_{ai}) - E = V_+(R_{ai}) - H, \quad (1)$$

where $V_*(R)$ and $V_+(R)$ are, respectively, the potential energy functions for the Ne*-Ar and Ne-Ar⁺ systems and H is the height of the centrifugal barrier, namely the long range maximum of $[V_+(R) + E(b/R)^2]$. It follows that the probability for associative ionization is given by²²

$$P_A(E, b) = \exp \left[- \int_{R_{ai}}^{\infty} \Gamma(R) dR / \hbar v_r \right] \times \left\{ 1 - \exp \left[- 2 \int_{R_o}^{R_{ai}} \Gamma(R) dR / \hbar v_r \right] \right\}, \quad (2)$$

where R_o is the classical turning point and v_r is the radial velocity,

$$v_r = \left\{ \frac{2}{\mu} \left[E \left(1 - \frac{b^2}{R^2} \right) - V_*(R) \right] \right\}^{1/2}$$

with μ as the reduced mass of the system. The cross section for associative ionization is then given by

$$\sigma_A(E) = 2\pi \int_0^{\infty} P_A(E, b) b db. \quad (3)$$

Assuming $H = 0$, it is possible, at a given collision energy, to find tentatively the value of R_{ai} which accounts for the experimental branching ratio and, therefore, using Eq. (1), the corresponding $V_+(R_{ai})$ value. Pesnelle *et al.*²² have applied this procedure to the analysis of the branching ratios in He*-Ar ionization. For this system, whose cross sections have been measured with state selection, the assumption of a single incoming channel is valid, while in the outgoing channel three potential curves could be involved for the HeAr⁺ ion product ($^2\Sigma_{1/2}$, $^2\Pi_{3/2}$, $^2\Pi_{1/2}$).²⁴ The final ionic products for the Ne*-Ar system²⁵ are represented by the same sequence of states as in the HeAr⁺ ion, but the incoming channel appears more complicated. However Gregor and Siska have satisfactorily reproduced their differential elastic cross sections using only one potential energy curve. In fact anisotropy effects for this system are expected to be relevant only at short distances.^{11,26} In this range the $V_*(R)$ and $\Gamma(R)$ they obtained must be regarded as phenomenological average functions, which however can be considered suitable for a description of the collisions of unselected Ne* atoms with Ar.

In a first step we have applied the procedure used by Pesnelle *et al.* and described above, using the $V_*(R)$ potential curve by Gregor and Siska and the $\Gamma(R)$ function obtained as described in Sec. III A. In Fig. 6 the $V_+(R_{ai})$ values obtained from the analysis of the present data are reported. The results show a minimum around 2.5 \AA with a $V_+(R_{ai})$ value very close to the dissociation energy of 0.079 ± 0.004 eV experimentally determined from photoionization spectroscopy by Pratt and Dehmer²⁵ for the $^2\Sigma_{1/2}$ state of the NeAr⁺ ion. This can be considered as an indication that, at high collision energy, a large amount of the ionization events occurs through the ground state of the NeAr⁺ ion.

In order to take into account the presence of three states of the product NeAr⁺ ion, in a second step we have analyzed the branching ratio data introducing a modification in the above model.

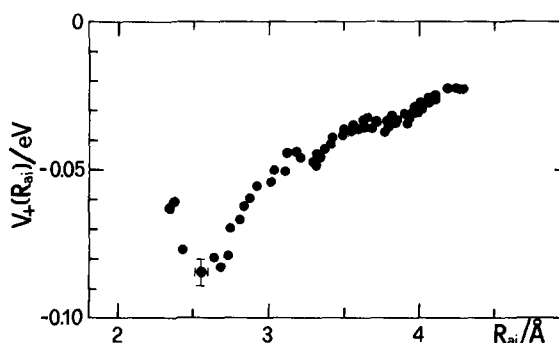


FIG. 6. Values of $V_+(R_{ai})$ obtained from the analysis of the branching ratios, neglecting the centrifugal barrier (see the text).

The three possible states $|J, \Omega\rangle$ of the NeAr⁺ ion, $|3/2, 1/2\rangle$, $|3/2, 3/2\rangle$, and $|1/2, 1/2\rangle$, are adiabatically connected, respectively, with the $^2\Sigma_{1/2}$, $^2\Pi_{3/2}$, and $^2\Pi_{1/2}$ states. Following recent theoretical work,²⁷ the electrostatic interaction can be represented by a spherical component V_0 and an anisotropic component V_2 both dependent on the interatomic distance. These two components are related to the usual V_Σ and V_Π interactions by

$$V_0 = \frac{1}{3}(V_\Sigma + 2V_\Pi)$$

and

$$V_2 = \frac{2}{3}(V_\Sigma - V_\Pi).$$

For the three NeAr⁺ states we can define three adiabatic potential energy curves²⁸

$$V_{|3/2, 1/2\rangle} = V_0 + \frac{1}{10}V_2 + \frac{1}{2}\Delta - D, \quad (4a)$$

$$V_{|3/2, 3/2\rangle} = V_0 - \frac{1}{3}V_2 \quad (4b)$$

$$V_{|1/2, 1/2\rangle} = V_0 + \frac{1}{10}V_2 + \frac{1}{2}\Delta + D, \quad (4c)$$

where

$$D = \frac{1}{10}(25\Delta^2 - 10V_2\Delta + 9V_2^2)^{1/2},$$

and Δ is the Ar⁺ spin orbit splitting. Using these equations an estimate of the potential energy curves of the NeAr⁺ ion has been obtained. The potential energy curve for the $|3/2, 3/2\rangle$ state, that is the pure Π state, has been obtained adding to the energy of the ground state NeAr dimer²⁹ the charge-induced dipole term given by $e^2\alpha/2R^4$, where α is the neon polarizability.³⁰ The $|3/2, 1/2\rangle$ state has been described by a Morse function connected at long range with the charge-induced dipole term through a cubic spline function: for the Morse branch an energy minimum equal to the experimentally determined value²⁵ at an equilibrium distance of 2.5 Å has been assumed. This value is near to that one corresponding to the minimum of $V_+(R_{ai})$ in Fig. 6 and higher than the limit of 2.45 Å which accounts for a dissociation energy given completely by the charge-induced dipole term only.²⁵ The $|1/2, 1/2\rangle$ state energy curve was derived using the above forms for the $|3/2, 3/2\rangle$ and $|3/2, 1/2\rangle$ curves to determine V_0 and V_2 and then substituting into Eq. (4c). This curve has a value of $(\Delta - 0.022)$ eV around 3.5 Å, in agreement with the experimental determination of Pratt and Dehmer.²⁵ In Fig. 7 the three potential energy curves are reported together with the corresponding three branching ratios calculated assuming that the ionization leads exclusively to one of the NeAr⁺ states.

The branching ratio calculated by an appropriate combination of the cross sections for the three final states is also reported in the figure. The weighting coefficient for each state has been assumed equal to the relative amount of Σ character of the state,³¹ following the suggestion by Morgner¹³ about a propensity of the system to produce ions with a Σ symmetry. Obviously the $|3/2, 3/2\rangle$ state, which is a pure Π state, has a coefficient of zero for all distances, while at long range, for the $|3/2, 1/2\rangle$ and $|1/2, 1/2\rangle$ states, the coefficients have, respectively, the statistical values of 2/3 and 1/3, which become 1 and 0 at short distances, where Λ is a good quantum number and therefore the two states are, respectively, pure Σ and Π states. The agreement at high collision energy between the calculated and experimental

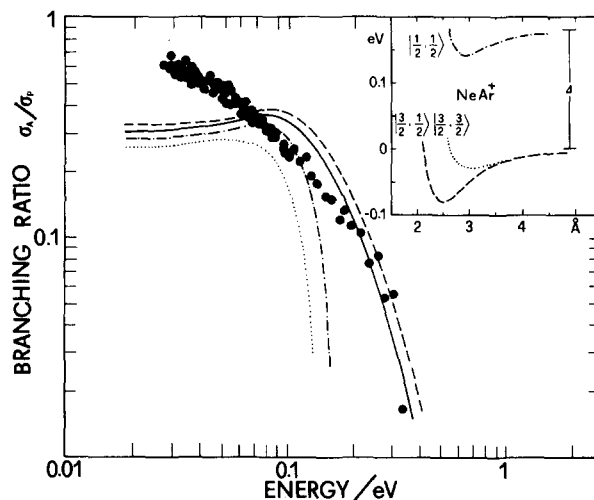


FIG. 7. Branching ratios as calculated using for the final NeAr⁺ states the potential energy curves shown in the window (see the text). The full line is the branching ratio obtained combining the states under the assumption that ions with Σ symmetry are formed.

branching ratios seems to support, for this energy region, that the ionization produces ions with Σ symmetry. However it must be noted that in the high energy limit the ions are formed at short internuclear distances where Λ starts to become a good quantum number. Therefore, in this energy region, ions with Σ symmetry are almost completely ions in the $^2\Sigma_{1/2}$ ground state.

The situation appears quite different at low collision energies where this model fails to reproduce satisfactorily the experimental results. We have tried to fit the experimental data using several potential energy curves for the final ion, but it has been impossible to find realistic curves which allow a satisfactory description of the branching ratio in the whole energy range experimentally investigated. In our opinion one of the possible explanations could be a poor adequacy of the "classical" model in the low collision energy limit. Another possibility could involve different ionization mechanisms at different energies.

C. Some considerations on the ionization mechanism

Following the classical model²⁰ it is possible to study which ranges of the impact parameters and of the internuclear distance are mainly contributing to the ionization. In Fig. 8 the probability for total ionization²⁰

$$P_T(E, b) = 1 - \exp \left[-2 \int_{R_0}^{\infty} \Gamma(R) dR / \hbar v_r \right]$$

is plotted as a function of the impact parameter, for three different collision velocities. In the same figure the contribution to the total ionization cross section $2\pi b P_T(b)$ is also reported as a function of b , and of the corresponding turning point R_0 . Taking into account that the ionization mainly occurs around R_0 where $v_r = 0$, Fig. 8(c) gives an idea of the effective contribution to the ionization as a function of the internuclear distance. A long range tail can be observed which is somewhat larger than that expected for He⁺-Ar system.³²

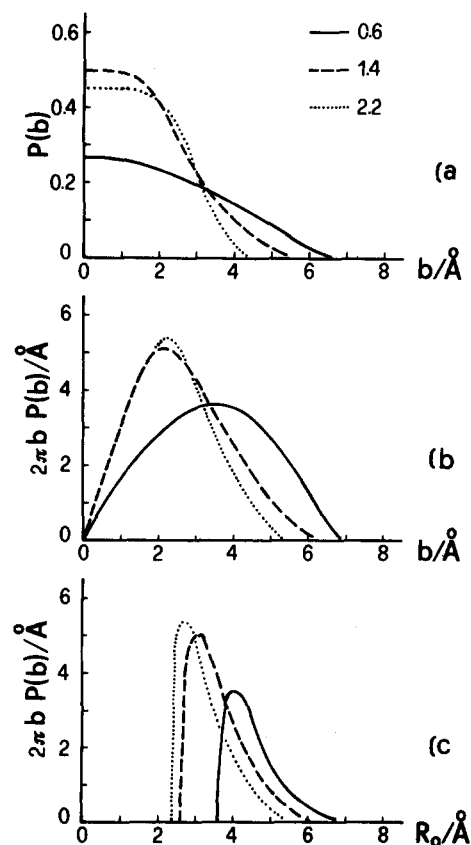


FIG. 8. Total ionization probability as a function of the impact parameter (a). The contribution to the total ionization cross section, $2\pi b P_T(b)$, is reported as a function of the impact parameter (b) and of the turning point (c). The curves are for three collision velocities: 0.6, 1.4, and 2.2 km/s.

An important aspect of the present system is the P -state nature of the Ne* atom. In fact an interesting problem about these ionization processes is the role played by the interaction anisotropy between the reacting partners. The collisions between P -state atoms and ground state rare gas atoms have been the object of several theoretical and experimental studies.¹² Aquilanti and Grossi²⁷ have recently proposed the use of the Hund's cases to describe the collision dynamics for these systems. To study the state of the collision partners just before the ionization event the decoupling schemes of Aquilanti *et al.*³³ have been applied. In Fig. 9 the schematic correlation between the J , Ω , and Λ states for the Ne* ($^3P_{2,0}$)-Ar system is shown. An estimate of the Σ - Π splitting can be obtained, as suggested by Gregor and Siska, from that of Ar- F ³⁴ scaled downward by a factor ~ 3 .¹¹ For collision velocities from 0.4 to 2.2 km/s, the centrifugal coupling terms $2\hbar vb/R_0^2$,²⁷ at the turning point corresponding to those impact parameters leading to ionization, are plotted in Fig. 10 and compared with the $(V_\Sigma - V_\Pi)$ values. In the present collision energy range, the spin-orbit splitting of Ne* is always larger than $(V_\Sigma - V_\Pi)$, therefore in thermal energy collisions Λ can never be considered as a good quantum number. At distances where the centrifugal term is smaller than the Σ - Π splitting, the system is described by the Hund's case (c), i.e., Ω is a good quantum number. On the other hand at larger distances where the centrifugal term is larger than the Σ - Π splitting, the system is described by the

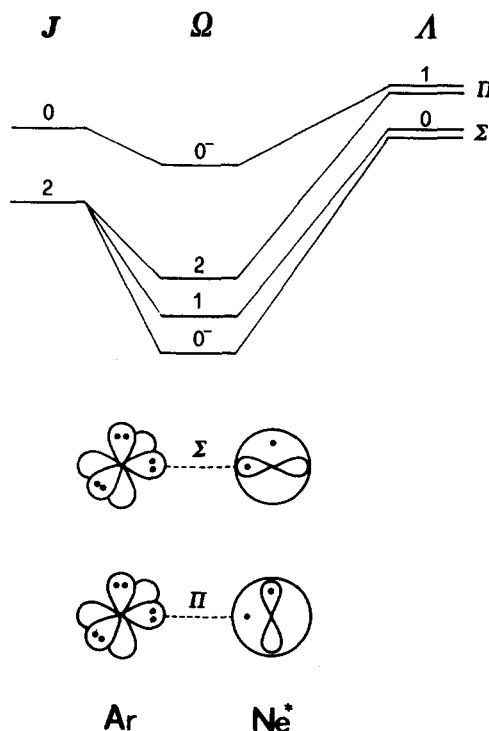


FIG. 9. Schematic correlation between the J atomic states of Ne*-Ar system, with the Ω and Λ states, respectively, for intermediate and short interatomic separation. In the lower part, the orientation of the 2p half-filled orbital of the Ne* atom respect to the internuclear axis for the Σ and Π symmetries is schematically shown.

Hund's case (e). In this region neither Λ nor Ω are good quantum numbers and the system is characterized by the states of the individual separated atoms. From the figure it appears that a large amount of the ionization events occurs

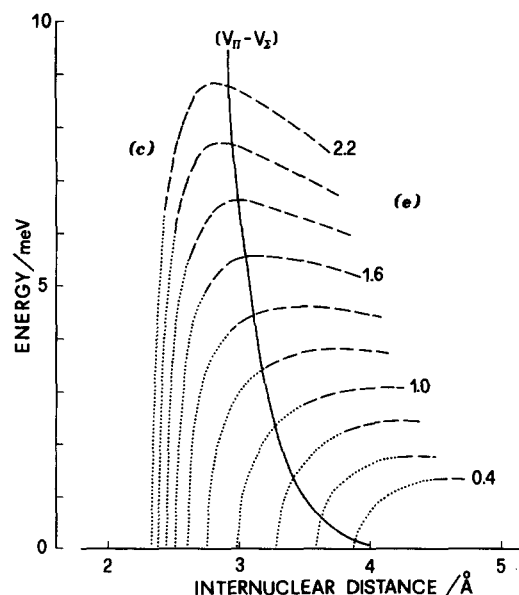


FIG. 10. Centrifugal coupling terms in Ne* ($^3P_{2,0}$)-Ar collisions, as dotted line for distances where associative ionization occurs and as dashed line for distances where Penning ionization occurs. The numbers indicate the collision velocity in km/s. The continuous line is the Σ - Π splitting and this curve separates the region of the Hund's case (c) from that of the Hund's case (e).

when the state of the two reacting atoms is described by the Hund's case (e), especially at low collision velocities.

It has been shown theoretically³⁵ that for the Penning and associative ionization two mechanisms are possible: one is called "exchange" mechanism and the other one "radiative". The exchange mechanism involves a transfer of the outer shell electron of the target into the inner shell vacancy of the metastable atom with the consequent ejection of the external excited electron. The radiative mechanism involves a deexcitation of the metastable atom with the emission of a virtual photon which ionizes the target. The exchange mechanism is expected to be affected, in a first approximation, by the overlap between the outer shell orbital of the target and the half-filled inner shell orbital of the metastable atom. On the other hand the radiative mechanism is expected to be influenced by the polarization of the metastable outer shell orbital due to the interaction with the target. For He*-rare gas systems it has been shown that the radiative contribution to the ionization does not play a significant role, but the dominant mechanism is the exchange one.³¹ On the basis of a simple one-electron calculation, Gregor and Siska¹¹ have suggested the possibility that in the present system the radiative mechanism contribution to the ionization cannot be neglected. As we observed, the Ar ionization by Ne* atom collision can occur at so large interatomic distance that the system is described by the Hund's case (e). This reasonably implies a weak overlap between the half-filled 2p orbital of Ne* and one of the 3p Ar orbitals and therefore implies, for this range, a small contribution of the exchange mechanism supporting the suggestion of Gregor and Siska.

IV. CONCLUSION

In spite of the poor adequacy of the two models to describe in the whole energy range the experimental Penning to associative ionization branching ratio, it appears that at high values of the investigated collision energies the ionization occurs mainly through the $^2\Sigma_{1/2}$ state of the NeAr⁺ ion.

Some considerations about the angular momenta coupling of the two reacting atoms, during the ionization event, allows to reach some interesting conclusions about the role played by the interatomic interaction anisotropy. In the low energy limit (≤ 15 meV) the ionization occurs with the reactants completely in the Hund's case (e), therefore the system is expected to behave isotropically, and the ionization should be insensitive to the Ne* J state. Going to higher energies the system is expected to show more and more an anisotropic behavior. It follows that a different ionization mechanism at different collision energies could be possible.

The considerations about the role of the anisotropy are also supported by a very recent experiment performed at Eindhoven,³⁶ where the energy dependence of the total ionization cross section for Ne* + Ar, Kr, and Xe has been measured with J selection. The results show that the Ne*(3P_2)-Ar and Ne*(3P_0)-Ar cross section ratio tends to unity going to the low energy limit. Valuable information for a deeper understanding of these processes could be obtained in the future by a combined analysis of the differential³⁷ and the integral scattering cross sections measured with state selected Ne* beams together with the corresponding Penning and

associative ionization cross sections as a function of the collision energy.

ACKNOWLEDGMENTS

The authors like to thank V. Aquilanti and F. Pirani for helpful discussions. Critical comments by H. Hotop and V. Kemper are also gratefully acknowledged. This research has been accomplished with a financial support of the "Italian National Research Council" (C.N.R.). Part of this work has been financially supported by the Philips Research Laboratories (The Netherlands). A.G.N. is grateful to the "Generalitat de Catalunya" (Spain) which, through the C.I.R.I.T. has afforded his stay in Italy.

- ¹For a recent review see: A. Niehaus, *Adv. Chem. Phys.* **45**, 399 (1981).
- ²See for instance: W. Lindinger, A. L. Schmeltekopf, and F. C. Fehsenfeld, *J. Chem. Phys.* **61**, 2890 (1974).
- ³R. D. Taylor and J. B. Delos, *Proc. R. Soc. London Ser. A* **379**, 179 (1982).
- ⁴W. P. West, T. B. Cook, F. B. Dunning, R. D. Rundel, and R. F. Stebbings, *J. Chem. Phys.* **63**, 1237 (1975).
- ⁵V. Cermak and J. B. Ozenne, *Int. J. Mass Spectrom. Ion Phys* **7**, 399 (1971).
- ⁶S. Y. Tang, A. B. Marcus, and E. E. Muschlitz, Jr., *J. Chem. Phys.* **56**, 566 (1971).
- ⁷D. A. Micha, S. Y. Tang, and E. E. Muschlitz, Jr., *Chem Phys Lett.* **8**, 587 (1971).
- ⁸R. E. Olson, *Chem. Phys. Lett.* **13**, 307 (1972).
- ⁹R. H. Neynaber and G. D. Magnuson, *Phys. Rev. A* **11**, 865 (1975).
- ¹⁰R. H. Neynaber and G. D. Magnuson, *Phys. Rev. A* **14**, 961 (1976); R. H. Neynaber and S. Y. Tang, *J. Chem. Phys.* **70**, 4272 (1979).
- ¹¹R. W. Gregor and P. E. Siska, *J. Chem. Phys.* **74**, 1078 (1981).
- ¹²See for instance: V. Aquilanti, G. Grossi, and F. Pirani, in *Electronic and Atomic Collisions*, Invited papers and progress reports, XIII ICPEAC (North-Holland, Amsterdam, 1983), p. 441 and references therein.
- ¹³H. Morgner, *Comments At. Mol. Phys.* **11**, 271 (1982).
- ¹⁴H. Hotop, J. Lorenzen, and A. Zastrow, *J. Electron Spectrosc. Relat. Phenom.* **23**, 347 (1981).
- ¹⁵L. Kaufhold, Diplomathesis, University of Freiburg, 1975; K. Gerard, Diplomathesis, University of Freiburg, 1976.
- ¹⁶C. H. Chen, Ph. D. thesis, University of Chicago, 1974.
- ¹⁷A. Aguilar, B. Brunetti, M. Cardinalini, F. Vecchiocattivi, and G. G. Volpi, *Gazz. Chim. Ital.* **113**, 711 (1983).
- ¹⁸R. B. Bernstein, *Comments At. Mol. Phys.* **4**, 43 (1973).
- ¹⁹J. M. Brom, J. H. Kolts, and D. W. Setser, *Chem. Phys. Lett.* **55**, 44 (1978).
- ²⁰W. H. Miller, *J. Chem. Phys.* **52**, 3563 (1970).
- ²¹C. H. Chen, H. Haberland, and Y. T. Lee, *J. Chem. Phys.* **61**, 3095 (1974).
- ²²A. Pesnelle, G. Watel, and C. Manus, *J. Chem. Phys.* **62**, 3590 (1975).
- ²³A. P. Hickman and H. Morgner, *J. Phys. B* **9**, 1765 (1976).
- ²⁴P. M. Dehmer, *Comments At. Mol. Phys.* **13**, 205 (1983).
- ²⁵S. T. Pratt and P. M. Dehmer, *J. Chem. Phys.* **76**, 3433 (1982).
- ²⁶M. A. D. Fluendy, I. H. Kerr, and K. P. Lawley, *Mol. Phys.* **28**, 69 (1974).
- ²⁷V. Aquilanti and G. Grossi, *J. Chem. Phys.* **73**, 1165 (1980).
- ²⁸V. Aquilanti, E. Luzzatti, F. Pirani, and G. G. Volpi, *Chem. Phys. Lett.* **90**, 382 (1982).
- ²⁹R. Candori, F. Pirani, and F. Vecchiocattivi, *Mol. Phys.* **49**, 551 (1983).
- ³⁰A. Dalgarno and A. E. Kingston, *Proc. R. Soc. London Ser. A* **259**, 424 (1960).
- ³¹V. Hoffmann and H. Morgner, *J. Phys. B* **12**, 2857 (1979).
- ³²S. Burdinski, R. Feltgen, F. Lichterfeld, and H. Pauly, *Chem. Phys. Lett.* **78**, 296 (1981).
- ³³V. Aquilanti, P. Casavecchia, G. Grossi, and A. Laganà, *J. Chem. Phys.* **73**, 1173 (1980).
- ³⁴V. Aquilanti, E. Luzzatti, F. Pirani, and G. G. Volpi (to be published). This Σ - Π splitting has been obtained for Ar-F system from scattering data of magnetically polarized atoms (see Ref. 12).
- ³⁵W. H. Miller, and H. Morgner, *J. Chem. Phys.* **67**, 4923 (1977).
- ³⁶H. C. W. Beijerinck (private communication); M. J. Verheijn, Doctoral Thesis, Technische Hogeschool Eindhoven, 1984.
- ³⁷W. Beyer, H. Haberland, and D. Hausamann, *IX International Symposium on Molecular Beams* (Freiburg, 1983), Book of Abstracts, p. 229.